HHS Public Access

Author manuscript

Ecotoxicol Environ Saf. Author manuscript; available in PMC 2023 March 22.

Published in final edited form as:

Ecotoxicol Environ Saf. 2023 March 15; 253: 114649. doi:10.1016/j.ecoenv.2023.114649.

Evaluation of pancreatic δ- cells as a potential target site of graphene oxide toxicity in Japanese medaka (*Oryzias latipes*) fish

Asok K. Dasmahapatra[a,b], **Paul B. Tchounwou**[a,*]

[a]RCMI Center for Environmental Health, Jackson State University, Jackson, MS 39217, USA

[b]Department of BioMolecular Sciences, Environmental Toxicology Division, University of Mississippi, University, MS 38677, USA

Abstract

In continuation to our previous investigations on graphene oxide (GO) as an endocrine disrupting chemical (EDC), in the present experiment, we have investigated endocrine pancreas of Japanese medaka adults focusing on δ-cells in the islet organs as an endpoint. Breeding pairs of adult male and female fish were exposed to 0 mg/L (control) or 20 mg/L GO by continuous immersion (IMR) for 96 h, or to 0 μg/g or 100 μg/g GO by a single intraperitoneal (IP) administration and depurated 21 days in a GO-free environment. Histological investigations indicated that the endocrine cells are concentrated in one large principal islet, and several small secondary islets scattered within the mesentery near the liver and intestine. The cells of the islet organ are in various shapes with basophilic nuclei and eosinophilic cytoplasm. Immunohistochemical evaluation using rabbit polyclonal anti-somatostatin antibody indicated that immunoreactivity is localized either at the periphery or at the central region in principal islets, and throughout the secondary islets, and found to be enhanced in fish exposed to GO than controls. The soma of δ-cells exhibits neuron-like morphology and have filopodia like processes. Cell sorting as non-communicating δ-cells (NCDC), communicating cells (CC), and non- δ-cells (NDC) indicated that within an islet organ, the population of NDCC is found to be the least and NDC is the highest. Our data further indicated that GO-induced impairments in the islet organs of medaka pancreas are inconsistent and could be affected by the exposure roots as well as the sex of the fish.

*Correspondence to: RCMI Center for Environmental Health, Jackson State University, 1400 JR Lynch Street, Jackson, MS 39217, USA. paul.b.tchounwou@jsums.edu (P.B. Tchounwou).

Declaration of Competing Interest

The authors declare that they have no known competing financial interests or personal relationships that could have appeared to influence the work reported in this paper.

CRediT authorship contribution statement

Asok K Dasmahapatra: Conceptualization, Formal analysis, Investigations, Methodology, Project administration, Writing – original manuscript; **Paul B. Tchounwou:** Conceptualization, Funding acquisition, Project administration, Resources, Supervision, Writing and editing manuscript.

Appendix A. Supporting information

Supplementary data associated with this article can be found in the online version at doi:10.1016/j.ecoenv.2023.114649.

Keywords

Islet organ; Cell sorting; Endocrine disruptors; Immunohistochemistry; Toxicity; Histology

1. Introduction

At the onset of 21st century, due to the rapid growth of high throughput technology in medicine, engineering, agriculture, and material sciences, many new chemical compounds are generated and thereby a probability of disposal into the environment. Many of these compounds are probable endocrine disruptors, targeting endocrine organs and affect the health and life status of living organisms. The World Health Organization (WHO) enlisted 176 compounds synthesized from petrochemistry as potential endocrine disruptors (ED) that induced disorders in the structures and functions of the endocrine organs as well as hormonal functions in animal, either directly or indirectly (Seralini and Jungers, 2021). Recently, over 600 compounds have been enlisted in a database as endocrine disrupting chemicals (EDC) with reported evidence on humans and rodents (Karthikeyan et al., 2019). Even though considerable efforts are made by several regulatory agencies like US Environmental Protection Agency (USEPA), Organization of Economic Cooperation and Development (OECD), European Union (EU), and others, a vast majority of chemicals have not yet been properly assessed for their potential impact on the endocrine systems and also we are still witnessing uncontrolled introduction of many of the new compounds into the global environment (Krimsky, 2017). The engineered nanomaterial (ENM) graphene oxide (GO), an oxidized derivative of graphene (an allotrope of carbon), due to its 2D morphology and chemical stability has been extensively used in industries, and human health (Avant et al., 2019; Dasari et al., 2019, Li et al., 2020). In 2021, an estimated 820 k mt of graphite are produced in China alone and Turkey is the leading country in graphite reserve. Moreover, in 2021, US carbon fiber and graphene industry generated $1.68 billion as revenue and more than 6000 people in the USA were employed in carbon fiber and graphene manufacturing industries (Fernandez, 2022). As new technologies emerge, in the coming decades, due to low production cost of graphene, these numbers are expected to increase. Inevitably, graphene nanomaterials are released into the environment during manufacturing, transportation, and public use (De Marchi et al., 2018).

When released into the aquatic ecosystem, graphene nanomaterials will interact with a variety of biotic (plants, animals, and microbes) and abiotic (sunlight, temperature, nutrients dissolved in water) factors and have a possibility of significant degradation that impacted the aquatic habitats including fish (De Marchi et al., 2018; Han et al., 2019; de Medeiros et al., 2020). Despite the degradation and significant variation within the different layers of a water body, a recent investigation by the Water Quality Analysis Simulation Program 8 (WASP8; USEPA, www.epa.gov), in four aquatic ecosystems (lakes and rivers) of the Southern United States, indicated significant accumulation of GO in the water columns (ranged from 23 ± 1 ng/L to 8.3 μg/L), surface sediments (ranged from $5.2 \pm 6 \times 10^{-3}$ ng /kg to 1.6×10^{4} ng/kg±2 $\times 10^{2}$ ng/kg), and in deep sediments (2.5×10^{-3} ng/kg ± 2×10^{-5} ng/kg to 2.1×10^{2} ng/kg ± 4 ng/kg). The estimated time required to reduce the sediment nanomaterial concentrations by 50% for lakes are 37 + years and for rivers are 1–4 years (Avant et al., 2019). Such

prolonged deposition of GO in the aquatic ecosystem have induced adverse effects on aquatic lives. Therefore, it is necessary to evaluate the toxic potential of GO in all possible ways using multiple physical, chemical, and biological techniques and models. Until now, several studies indicated that the aquatic animals are sensitive to GO, and the toxic effects of the nanomaterial (GO) needs further in-depth studies and confirmation (dAmora et al., 2017, 2019).

For the past several years, significant efforts have been made by OECD, USEPA, EU, and others, to develop strategies for screening and identifying EDCs using model organisms living in different ecosystems (OECD, 2018). Our laboratory has been evaluating GO, as a potential EDC using Japanese medaka fish (*Oryzias latipes*) as the experimental model (Dasmahapatra et al., 2020a; b; Myla et al., 2021a; b; Asala et al., 2021, 2022; Dasmahapatra and Tchounwou, 2022a; b). Our studies demonstrated that the medaka males are more sensitive to GO than the females (Dasmahapatra et al., 2020a; b). From our histopathological evaluation of the gonadal structures, thyroid follicles, and interrenal glands (adrenal homolog in mammals) we found that the damages observed after GO administration, despite oxidative stress (Fernandez et al., 2018; Dasmahapatra et al., 2019, review), was mainly due to aggregation/agglomeration of GO on or within the organs rather than directly acting as an EDC (Dasmahapatra et al., 2020a; b; Myla et al., 2021a; b). Our investigations on the sex reversal (SR) of medaka larvae by GO showed no apparent EDC effect (Myla et al., 2021a; b). In the present study, we have extended our investigations on endocrine pancreas (islet organs), which could be a potential target endocrine organ for evaluation of GO as an EDC. To our knowledge this is the first report that the endocrine pancreas of a fish model is used to evaluate GO as an EDC. Consequently, we think that this study will probably fill in the gap that the endocrine pancreas should have potential as an endpoint organ in EDC evaluation. We hypothesized that if accumulated in medaka the effects of GO on the islet organs are sex-specific and depends on the route of exposure. As a result, endocrine-related cellular regulations in glucose metabolism controlled by the pancreas will be disrupted. Although it is too early to say that our observations on Japanese medaka will be helpful in using graphene nanoparticles for the treatment of diabetes or used as a drug-carrier, our studies will fill the gap that whether islet organs of the endocrine pancreas of Japanese medaka should be considered as a potential target organ of EDCs or not? Therefore, our major objective of the work is to identify a GO-sensitive cell in the endocrine pancreas of Japanese medaka that have significant impact on glucose metabolism of the fish. With this regard, we choose to characterize somatostatin-producing δ-cells which have significant impact on both insulin (secreted by β-cells) and glucagon (secreted by α-cells) producing cells within the organ and due to the presence of axon-like processes, these cells (δ-cells) can easily be separated from the round/oval shaped α- and β-cells by immunohistochemical staining using specific antibody. To test our hypothesis, we exposed the adult fish to GO either by 96 h continuous immersion (IMR) or by a single intraperitoneal (IP) injection and have concentrated on δ-cells after identifying them by immunohistochemical technique using rabbit generated polyclonal antisomatostatin antibody as primary antibody.

2. Materials and methods

All the experimental animal protocols (# IBC 08–01–17 and IBC 09–01–17) were approved by the Institutional Animal Care and Use Committee (IACUC) of the Jackson State University, Jackson, Mississippi, USA.

2.1. GO preparation

The procedure of GO synthesis, dilution, sonication, application to the animal was described previously (Dasmahapatra et al., 2020a; b, Dasmahapatra and Tchounwou, 2022a; b). Briefly, the GO used in the experiment was either synthesized in the laboratory and dispersed in the nanopure water at a concentration of 2 mg/mL (Dasmahapatra et al., 2020a; b) or obtained from a commercial source (2 mg/mL dispersed in water; Sigma-Aldrich, St. Louis, MO, USA;). Before used in the exposure, GO was sonicated for 5 min (2 s on-1 s off pulse, 225 w) using a probe sonicator (ultrasonicator LPX 750, Cole Palmer, Chicago, IL, USA) in ice temperature. The sonicated nanomaterial was further checked by TEM at the Electron Microscopy Core laboratory at the Jackson State University, Jackson, MS, USA (Dasmahapatra et al., 2020a; b). For IP studies the sonicated GO was injected directly (1 μL/10 mg fish) to the peritoneal cavity of the fish; for IMR studies, the sonicated GO was diluted to desired concentration (20 mg/L; 100-fold dilution) in balanced salt solution (BSS; 17 mM NaCl, 0.4 mM KCl, 0.3 mM $MgSO_4$, 0.3 mM $CaCl_2$, pH 7.4).

2.2. Animal maintenance and GO exposure

2.2.1. Test fish—The Japanese medaka fish colony (Orange red variety, Hd-rR strain) maintained at the Jackson State University, Jackson, MS, USA was described previously (Dasmahapatra et al., 2020a; b). Briefly, the adult fish used as breeders were maintained in 35 L tanks in 25 L BSS at 25 ± 1 ° C with 16 h L: 8 h D light cycle. The medium was recirculated through pumps and filtered through disposable bio and carbon filters. Depending on the pH (6.5–8.5) and ammonia concentrations (1–3 ppm), BSS was refreshed every two to three weeks, if necessary. The fish were fed twice daily with Tetramin flake and brine shrimp nauplii (morning feeding was in between 8 and 30–10–30 a.m. and afternoon feeding was in between 2 and 30–4–30 p.m.). The total length of the brooder during breeding was 3–3.5 cm and the body weight for males were 304.2 ± 11.04 mg (n = 46) and for females 384.3 ± 11.83 mg (n = 58) (Dasmahapatra et al., 2020b). The fish breed successfully in the 35 L tanks spontaneously in these environmental conditions and the eggs were generally collected within 1–3 h after the light turned on. The eggs after gentle separation from the clutch and removal of the dead and unfertilized embryos, were reared in embryo-rearing medium (ERM; 17 mM NaCl, 0.4 mM KCl, 0.6 mM $MgSO_4$, 0.36 mM $CaCl_2$, pH 7.4) and generally hatched within 8–14-day post fertilization (dpf) at 25 ± 1 °C with 16 h L and 8 h D light cycle. The hatched larvae were initially reared in small 200 mL jars with BSS (8–10 larvae/jar/200 mL BSS) and fed with tiny pinch of flakes and brine shrimp nauplii two times daily (as per a.m. and p.m. feeding schedule) after 2–3 days post hatch (dph). When they were larger (approximately 10–15 mm in length or 25–30 mg in weight) the larvae were transferred to bigger containers (jars/tanks) and finally to 35 L tanks and used either as breeders for the maintenance of the colony in the laboratory or used in experiments as and when required.

2.2.2. Exposure of adult fish to GO by IP—The adult medaka fish we used for immunohistochemical evaluation of pancreatic islet organs (endocrine pancreas) after IP exposure were obtained from our previous GO experiments on Japanese medaka adults (Dasmahapatra et al., 2020a; b). Briefly, before exposure to GO by IP, the fish were randomly collected from the stock tanks (35 L), maintained as a breeding pair (one male and one female) in 500 mL BSS in 1 L glass jar in the laboratory conditions (25 ± 1 °C and 16 h light: 8 h dark Light cycle). When they breed successfully for one week (7 days), GO was injected IP (100 μg/g) to the fish (both males and females) and the controls (both males and females) were injected with nanopure water (vehicle); the maximum volume of the injected material was 1 μL/10 mg body weight (volume was adjusted to nearest 10 mg). Although in our previous studies (Dasmahapatra et al., 2020a; b) we have used 4 different doses of GO (25, 50, 100, and 200 μg/g), for evaluation of islet organs by immunohistochemistry, we have considered only 100 μg/g GO group for evaluation. Previously, we have observed that the lethality of GO in medaka is sex-specific and males are more sensitive to GO than females; the calculated LD_{50} after 21 days post administration by IP for males was 175.39 μg/g and for females 2901.2 μg/g (16.5-fold higher) that affects the normal breeding of the fish (the calculated LD_{50} as a breeding pair was 110.75 μg/g) (Dasmahapatra et al., 2020b). We therefore choose only those fish which were exposed to 100 μg/g GO by IP, which we think was very close to LD_{50} and ideal for evaluation of islet organs. Moreover, in IP experiments, fish were injected with 100 μg/g GO either synthesized in the laboratory (3 pairs survived as breeding pairs) or obtained from commercial source (4 pairs survived as breeding pairs) (Dasmahapatra et al., 2020b). To avoid movement during injection, the fish were anesthetized in 100 mg/L MS 222 in BSS (Readman et al., 2017), and after injection, returned to regular BSS for quick recovery. When the fish recovered completely from anesthesia (judged from normal swimming behavior), both male and female fish are returned to the respective tanks for continuation of breeding (same partners) and fed twice daily until the end of the experiment. After 21days depuration (post-exposure), the survived fish (7 breeding pairs survived with 100 μg/g GO and controls 20 pairs) were anesthetized in MS 222 (100 mg/L) and processed for immunohistochemistry (OECD, 2009).

2.2.3. IMR experiments—Like IP experiments, the adult medaka fish we used for evaluation of pancreatic islet organs (endocrine pancreas) after IMR exposure were also obtained from our previous GO experiments on Japanese medaka (Dasmahapatra et al., 2022a, b). In these experiments, we have used only one concentration of GO (20 mg/L) for exposure (96 h in GO with refreshing of media every 24 h and then depurated for 21 days in a GO-free environment). The selection of 20 mg/L concentration of GO for exposure was based on an observation made by Mullick Chowdhury et al. (2014) who used graphene nanoribbons and observed that the nanomaterial at this concentration (20 mg/L) can cross the chorion-barrier of the medaka embryos and induced toxicological effects (Mullick Chowdhury et al., 2014). In addition, we have conducted series of immersion experiments on Japanese medaka larvae (1 day post hatch) after exposing them with different concentrations of GO (2.5, 5.0, 10, and 10.0 mg/L) for 96 h with refreshing of media every day and observed that small black particles were accumulated in the gut of medaka in a concentration-dependent manner, however, the controls (no GO) have clean gut (Myla et al., 2021b).

For IMR experiments, like IP, reproductively active adult male and female fish randomly collected from the stock tanks (35 L) and were allowed normal breeding for one week in 1 L glass jars containing 500 mL BSS (1 male and 1 female). We have used 9 breeding pairs in our experiment. After successful breeding for one week, 4 breeding pairs were continued to maintain in BSS and served as controls (no GO), while other 5 pairs were exposed to GO (20 mg/L) in BSS by IMR. Before addition to the medium (BSS), the GO (2 mg/mL; Sigma-Aldrich, St. Louis, MO, USA) was sonicated for 5 min in ice temperature as we did for IP experiment and diluted with required volume (5 mL of stock [2 mg GO/mL] in 495 mL of BSS). For IMR experiments we have used GO obtained from Commercial source (Sigma-Aldrich, St. Louis, MO). The GO exposure was continued for 96 h with refreshing of media every 24 h. During exposure (4 days) and post-exposure periods (21 days) the fish were fed twice (as per a.m. and p.m. schedule with brine shrimp nauplii and Tetramin Flakes) and the collection of eggs from each experimental tank were continued. After required period of treatment (96 h), the fish were transferred to fresh BSS with no GO and maintained in clean 1 L glass jars for 21 days with refreshing of media every 24 h and continued egg collection until the end of the experiment (Dasmahapatra and Tchounwou, 2022a; b). After 21days depuration (post-exposure), the survived fish (all nine pairs; no death) were anesthetized in MS 222 (100 mg/L) and processed for immunohistochemistry (OECD, 2009).

2.3. Histology of pancreatic islets of medaka

The trunk region of the medaka fixed in 4% PFA containing 20 mM PBS for 48 h (changed once after 24 h), was washed thoroughly in water. The washed tissues were dehydrated in graded alcohols, cleared in xylene, embedded in paraffin (58–60 °C) and the serial sections at 5 μm thickness were cut in a manual rotary microtome (Olympus cut 4055). To determine the exact location of pancreas on glass slides after histological preparation some of the paraffin sections were stained in hematoxylin-eosin (HE) or Periodic acid Schiff (PAS) technique. For immunohistochemical detection of δ-cells in the islets we used rabbit generated polyclonal anti-somatostatitin antibody (Abcam, Waltham, MA, USA) as primary antibody. The digital images of the stained sections were taken in an Olympus CKX53 inverted microscope attached with a DP22 camera with CellSens software (Huntoptics &Imaging, Pittsburg, PA, USA). The islet organs in the pancreas of adult medaka are located adjacent to the liver and gall bladder having two types of islets: the principal or the primary islet and the secondary islet. The single principal islet is comparatively bigger (400–900 μm in diameter) than the multiple (2–5 in number) secondary islets (70–500 μm) (Otsuka et al., 2015). We have considered mainly the principal islet in our study, however, secondary islets were also evaluated and included in analysis when available. The images captured in different regions of the islet tissue (minimum three snaps are required to cover the entire region of the principal islets and only one snap required for secondary islets) were used for manually counting the islet organ cells including δ-cells and the area of that particular region under cell count was determined by imagej software (http://www.imagej.nih.gov/ij).

2.4. Immunohistochemistry of somatostatin

For specific location of the δ-cells in the islet organs of Japanese medaka adults, we have used immunohistochemical technique for the detection of somatostatin, the paracrine

regulator (inhibition) of both α- and β-cells within the pancreatic islets, secreted from the δ-cells (Rorsman and Huising, 2018; Arrojo e Drigo et al., 2019; Huising, 2020; Gao et al., 2021). We have standardized the technique in our laboratory by following the guidelines provided by Abcam (Waltham, MA, USA) and Vector laboratories (Burlingame, CA, USA). Briefly, tissue Section (5 μm thickness) on glass slides containing islet organs were deparaffinized and brought to tap water. A 40 min antigen unmasking (antigen retrieval) was done in citrate buffer (pH 6.0) at 85–90 ° C. After washing in 0.1 M phosphate buffered saline- tween 20 (PBST), for blocking the endogenous peroxidases and alkaline phosphatases, the sections were treated for 10 min with bloxall (Vector laboratories, Burlingame, CA, USA) at room temperature. After a brief wash with PBST, before the application of primary antibody, the sections were incubated for 1 h with 3% normal goat serum (Vector laboratories, Burlingame, CA, USA) at room temperature. Then the sections were incubated with primary antibody (polyclonal rabbit-derived anti-somatostatin antibody; Abcam, Waltham, MA) with a final dilution of 1:600 in 3% goat serum in PBST, left overnight at 4 °C. During standardization of the procedure, parallel control sections on glass slides were incubated in identical conditions in 3% goat serum-PBST without primary antibody. Sections were washed several times in PBST and incubated for 1 h at room temperature with biotinylated goat antirabbit secondary antibody (Vector laboratories, Burlingame, CA, USA) diluted (1:300) in PBS with 3% goat serum. Sections were washed again in PBS and incubated for 1 h at room temperature with avidin-biotin complex in PBS as recommended by the manufacturer (Vector laboratory, Burlingame, CA, USA). The sections were washed several times in PBS and incubated for 1 h at room temperature with vectastain elite ABC reagent (Vector laboratory, Burlingame, CA, USA). They were washed several times in PBS and incubated in room temperature for 5–10 min with freshly prepared peroxidase substrate (vector DAB) as recommended by the manufacturer (Vector laboratories, Burlingame, CA, USA). After incubation, they were also washed in tap water and counter stained with hematoxylin, dehydrated in alcohol, cleared in xylene, and mounted in permount (Fisher scientific; St. Louis, MO, USA). These sections were evaluated and photo-graphed under microscope (Olympus CKX53 inverted microscope attached with DP22 camera with CellSens software; Huntoptics&imaging, Pittsburg, PA, USA). Antibody positive cells (δ-cells) were deep brown in color (Fig. 2a, b), and the sections without primary antibody (Fig. 2c) did not show any reaction/brown color.

2.5. Evaluation of islet organs

After administration of GO, either by IP or IMR, we have allowed them 21 days for depuration as recommended in OECD guidelines (Test No 230: 21-day Fish Assay; OECD, 2009). Among the experimental fish, after immunohistochemical staining, due to technical problems, we can track the islet tissues of two control males and two control female fish exposed in BSS (96 h + 21days; no GO) as well as three males and three female fish exposed to GO (20 mg/L in BSS for 96 h and then depurated in fresh BSS for 21 day (96 h with GO+ 21 days no GO). Similarly, For IP experiments, we can track islet organs of only two control males and two control female fish (no GO), and three males and three female IP-injected fish with GO (100 μg/g GO, single IP injection) (Please see schematic diagram in Fig. 1 and supplementary Tables ST-1 and ST-2).

2.6. Evaluation of δ-cells in the islet organ

Although the islet organ of teleost fish consists of α-, β-, δ-, and ε-cells, in the present study, we have focused our investigations only on somatostatin secreting δ-cells, the paracrine regulator (inhibitory) of α- (glucagon) and β- (insulin) cells within the islet organs. Like in humans or mice, δ-cells in medaka, unlike α- and β-cells, exhibit neuron-like morphology with a well-defined cell soma and filopodia like processes (containing somatostatin) which can permit us to identify the immunopositive (positive to somatostatin antibody) δ-cells within the islets. However, the filopodia are highly plastic, showing rapid morphological changes and connect any of the neighboring cells (including α-, β-, and δ-cells) with these filopodia-like processes making the study more complex. To make it straight-forward, we have evaluated the effect of GO on δ-cells and developed a strategy with the use of digital photography and imagej software. The digital photographs of the different regions of islet organs were taken and all the islet organ cells (excluding blood cells) were manually counted in that particular region and classified into three categories (Fig. 3a,b and supplementary Tables ST-1 and ST-2); (i) non-communicating δ-cells (NCDC) in which the filopodia are positive to immunostaining, however, the filopodial ends (tips of the filopodia) did not directly communicate with any other δ-cells or non- δ-cells within the islet organ; (ii) the communicating cells (CC); these islet cells including δ-cells and other islet tissue cells (excluding blood cells), are associated with other immunoreactive cells or blood vessels either directly by filopodial connections or remained closely associated with filopodia without any visible connections within the islet, (iii) non- δ-cells (NDC); these cells (excluding blood cells) within the islet tissues are oval, round or elongated in appearance, devoid of filopodia like process and remained negative to immunostaining. The cell numbers were expressed as number of cells (NCDC, CC, or NDC)/ mm^2 of the islet organ (Tables ST-1 and ST-2). Our preliminary data indicated that when we compare all these three cell types considering all 20 experimental fish irrespective of sex (male/female), GO exposure (GO/no GO), or mode of exposure (IMR/IP), the population (%) of NCDC is found to be the least (14.46 ± 1.48, n = 20) and NDC is the highest (52.77 ± 3.19, n = 20) and CC population remained intermediate (32.76 ± 2.92, n = 20) between these two (Fig. 3b; ST-2).

2.7. Statistical analysis

Experimental data were analyzed using GraphPad prism version 7.04 (GraphPad Prism, San Diego, CA). We used descriptive analysis to evaluate nuclear area (μm^2) and filopodial length (μm) in NCDC and the distribution (number/mm^2) of NCDC, CC, and NDC, within the islet organ of Japanese medaka adults after immunohistochemical staining and digital photography. We used D′Agostino-Pearson (DP) or Shapiro-Wilks (SK) test to determine the normality of the data. However, our normality test on data did not meet the criteria of using a parametric test, we, therefore, performed the Kruskal-Wallis test followed by Mann-Whitney's test (nonparametric test) as a post-hoc test and the level of significance adopted as $p < 0.05$. All the numerical data were expressed as mean ± SEM.

3. Results

3.1. Histology of the islet tissue

The pancreas of medaka is located dorsally to the liver and near the extrahepatic common bile duct (Assouline et al., 2002) scattered in the mesentery. The pancreatic endocrine cells of Japanese medaka adults are concentrated in one large principal islet, and several smaller secondary islets scattered within the mesentery near the liver and gall bladder. The principal islet is in a more posterior region than secondary islets, which are scattered along the gut tube, sometimes close to the bile duct (Otsuka et al., 2015; Otsuka and Takeda, 2017). The histological studies by HE staining indicated that the cells of the islet tissue are round, oval, elongated or cylindrical in shape with basophilic nuclei and eosinophilic cytoplasm. Several blood vessels with blood cells are passing through the islet tissues (Fig. 4: supplementary Fig. SF-1). In PAS staining, several PAS positive regions were observed (Fig. SF-2). Both the staining techniques indicated several cells which have processes like delta cells (Figs. SF1, SF2).

3.2. Effect of GO exposure on the histological architecture of medaka pancreas after immunohistological staining

Although the islet tissue consists of at least four different kinds of cells, we have focused our study on δ-cells, which are considered as the intra-islet local paracrine regulator of α- and β-cells and a potent inhibitor of insulin and glucagon secretion (Gao et al., 2021). These cells are easily detected by antisomatostatin antibody (Figs. 2a–2c). Our studies indicated that immunoreactivity (antisomatostatin antibody) in principal islet is localized either at the periphery or at the central region, and in the entire islet tissue for the secondary islets (Figs. 2a–2b). Most α- and β- cells are rounded or rhomboid (nonreactive to antisomatostatin antibody, and therefore recognized after counterstaining in hematoxylin), however, the immunoreactive δ-cells showed more complex neuron-like morphology and have long, neurite- or filopodia-like processes (Fig. 3a–b; Fig. 5a–h) that can make close contact with α-, β-, and δ-cells at some distance from the cell body, thereby enabling excessive paracrine, endocrine, neuronal and nutritional inputs within an islet organ of the endocrine pancreas (Fig. 3a–b; Figs. 5a–5h). The effect of GO exposure on δ-cell architecture was also evaluated either exposed by IMR (Figs. 5a–5d) or by IP (Figs. 5e–5h) on male (Fig. 5a–b, Fig. 5e–f) and female (Fig. 5c–d, and Fig. 5g–h) fish. Although we are unable to detect any morphological abnormalities in δ- cells between control (Figs. 5a,5c, 5e,5g) and GO-exposed (Figs. 5b, 5d, 5f, 5h) fish, it appears that the immunoreactivity (somatostatin) in GO exposed fish either by IMR (20 mg/L) male (Fig5b) and female (Fig. 5d) or by IP (100 μg/g) male (Fig. 5 f) or female (Fig. 5 h) fish appears to be comparatively higher than the corresponding control male (Fig. 5a) and female (Fig. 5c) fish exposed in BSS (IMR) or in vehicle-injected IP (control) male (Fig. 5e) and female (Fig. 5 g) fish. Therefore, we have extended our investigation on cell counting in both principal and secondary islet organ cells (except blood cells) whether immunoreactive to antisomatostatin antibody or not and express the number of cells/ mm^2 of islet organ (Figs. 3a and 3b; Figs. 5a–5b;Tables ST1 and ST-2) after classifying them into three types; NCDC, CC, and NDC.

3.2.1. Noncommunicating delta cells (NCDC—Due to the presence of somatostatin-positive filopodia which appears to be unassociated in cell communication in these cell types, we can easily separate them (NCDC) from other cell types (CC and NDC) we studied in islet organs. Our data indicated that within an islet organ, these cells (NDCC) are least in number (14.46 ± 1.482%; n = 20) compared to other two cell types (CC and NDC) we have included during evaluation (Tables ST-1 and ST-2).

For comparison, we have analyzed the NCDC data based on the sex of the animal (male vs. female), mode of exposure of the fish to GO (IMR vs. IP) and the exposure of the fish to GO (no GO vs GO). Our data indicated that the nuclear area of NCDC in the control male fish exposed to BSS either alone (control) or with GO (20 mg/L) by IMR is not significantly different (NS) from the corresponding control female fish; (control male IMR vs. control female IMR, p = NS; 20 mg/L GO male IMR vs. 20 mg/L GO female IMR, p = NS); however, in IP-injected male fish either as control (no GO, vehicle only) or with GO (100 μg/g), the nuclear area was significantly higher in males than the females (control male IP vs. control female IP, $p < 0.05$; 100 μg/g GO male IP vs. 100 μg/g GO female IP, $p < 0.05$) (Fig. 6a.). When the comparison was made with regard to the mode of exposure (IMR vs IP), we have observed that the nuclei in both the control male and female fish in IMR have significantly higher area ($p < 0.05$) than the corresponding control male and female fish in IP (control male IMR vs control male IP, $p < 0.05$; control female IMR vs control female IP, $p < 0.05$); while, when the male fish exposed to GO either by IMR (20 mg/L) or IP (100 μg/g) did not show any significant difference in nuclear area (male fish in GO by IMR vs. male fish in GO by IP; p = NS), however, in females, the nuclear area appears to be significantly higher ($p < 0.05$) in fish exposed to GO by IMR than the fish (female) exposed to GO by IP (GO in female by IMR vs. GO to female by IP, $p < 0.05$) (Fig. 6a). Also, the effect of GO in the nuclear area of NCDC was observed in both male and female fish exposed to GO either by IMR or by IP. It was noticed that in IMR fish GO at 20 mg/L concentration significantly reduced the nuclear area of NCDC than control in both male and female fish (control male IMR vs. GO male IMR, $p < 0.05$; control female IMR vs. GO female IMR, $p < 0.05$), however, remained unaltered in IP fish (control male IP vs. GO male IP, p = NS; control female IP vs. GO female IP, p = NS) (Fig. 6a).

We have also evaluated the linear length (μm) of filopodia in these cells (NCDC) in male and female Japanese medaka fish exposed to GO either by IMR or IP (Fig. 6b). Our data indicated that the linear length of filopodia we can measure in the NCDC from all 20 experimental fish were highly variable (ranged from 0.81 to 11.95 μm; n = 787). Moreover, only the control male IMR fish showed significantly higher length of filopodia in NCDCs than the female fish immerse in BSS (control) (control male IMR vs. control female IP, $p < 0.05$), while, the male fish exposed to GO by IMR (20 mg/L) did not show any significant difference when compared with the corresponding female fish exposed to GO (GO male IMR vs. GO female IMR, p = NS). In IP fish, whether as control or exposed to GO (100 μg/g), the filopodial length in both male and female fish remained identical (control male IP vs. control female IP, p = NS; GO male IP vs. GO female IP, p = NS) (Fig. 6b). Considering the mode of exposure (IMR vs IP), the filopodial length in control male IMR fish did not differ significantly with the control male IP fish (control male IMR vs. control male IP, p

= NS), while the control female fish in IMR have significantly reduced filopodial length of NCDCs than the female IP fish (control female IMR vs. control female IP, $p < 0.05$). In contrast to the control fish, the male fish exposed to GO by IP (100 μg/g), have significantly higher length of filopodia in NCDCs than the male fish exposed to GO by IMR (GO male IMR vs. GO male IP, $p < 0.05$), while in females, the filopodial length of NCDC remained identical between the fish exposed to GO by IMR and IP (GO female IMR vs. GO female IP, p = NS) (Fig. 6b). The linear length of filopodia in NCDCs was further evaluated in the male and female fish exposed to GO either by IMR or IP. Our data indicated that compared to corresponding controls, IMR males did not show any significant difference with IMR males exposed to GO (control males IMR vs. GO males IMR, p = NS), however, significant enhancement in the linear length of filopodia was observed only in male fish exposed to GO (100 μg/g) by IP (control males IP vs. GO males IP, $p < 0.05$). In contrast to males, females, exposed to GO by IMR showed significant increase in the linear length of filopodia in NCDCs compared to controls exposed in BSS by IMR (control females IMR vs. GO females IMR, $p < 0.05$), while females in IP did not show any significant difference when compared with corresponding control female fish in IP (control female IP vs. GO female IP, p = NS) (Fig. 6b).

Our evaluation of the cellular distribution (number/ mm^2) of NCDCs within an islet organ of experimental medaka fish is presented in Fig. 6c. Our data indicated that the number of NCDCs in islet organs remained at the same level between control IMR male and female fish and between IP control male and female fish (IMR control male vs. IMR control female, p = NS; IP control male vs. IP control female, p = NS) (Fig. 6c). However, after exposure to GO by IMR, female fish have significantly greater number of NCDC compared to male fish exposed to GO by IMR (GO male IMR vs. GO female IMR, $p < 0.05$) (Fig. 6c). No significant difference was observed in NCDC numbers between male and female IP fish served either as control or GO (IP male control vs. IP female control, p = NS; GO male IP vs. GO female IP, p = NS) (Fig. 6c). When comparison was made between the mode of exposure to GO (IMR vs. IP), the control fish, either male or female did not show any significant difference in NCDC number between the fish exposed by IMR and IP (control male IMR vs. control male IP, p = NS; control female IMR vs. control female IP, p = NS). However, both male and female fish exposed to GO by IP (100 μg/g), showed a significant difference (increase) with the corresponding male and female fish exposed to GO by IMR (GO male IMR vs. GO male IP, $p < 0.05$; GO female IMR vs. GO female IP, $p < 0.05$) (Fig. 6c). Moreover, GO, either by IMR (20 mg/L) or by IP (100 μg/g) did not altered the NCDC number in the islet organs of both male and female medaka (Control male IMR vs. GO male IMR, p = NS; Control female IMR vs. GO female IMR, p = NS; control male IP vs. GO male IP, p = ns; control female IP vs. GO female IP, p = NS) (Fig. 6c).

3.2.2. Communicating cells—In our studies, the communicating cells (CC), we considered for evaluation, are those cells interconnected with the neighboring cells by filopodia or remained tightly associated with filopodia like processes (filopodia passes between these cells with the sign of immunoreactivity) (Fig. 3b). We have also observed that these cells (CC) were sometimes directly connected to the vascular network via filopodia (supplementary Figure SF-3). As the communicating cells are not absolutely δ-cells (α-,

β-, and other islet cells could be contributed) during evaluation, we have focused our studies only with the cellular distribution (number/mm^2) of CCs within the islet organs. Our data indicate that the number of CCs in male and female IMR fish served as controls did not differ significantly (control IMR male vs. control IMR female, p = NS), however, significantly less in number in control female IP fish than corresponding control IP males (control IP male vs. control IP female, $p < 0.05$) (Fig. 7a). Moreover, the male fish exposed to GO by IMR have significantly higher number of CC than the corresponding females, even though in IP male fish exposed to GO (100 μg/g), showed equal identity in CC numbers with female fish (IMR male GO vs. IMR female GO, $p < 0.05$; IP male GO vs. IP female GO, p = NS). With regard to mode of exposure (IMR vs IP), the control male and female in IMR have equal number of CCs with the corresponding control male and female in IP (control male IMR vs. control male IP, p = NS; control female IMR vs. control female IP, p = NS) (Fig. 7a); however, the males exposed to GO by IMR have significantly higher number of CC than the males exposed to GO by IP though the females exposed to GO by IMR have identical status in CC number compared with the females exposed to GO by IP (IMR male GO vs IP male GO, $p < 0.05$; IMR female GO vs. IP female GO, p = NS) (Fig. 7b). Comparison of the data to show the effects of GO on male and female medaka, the CCs in male fish exposed to GO by IMR have significantly higher in number than the corresponding control males exposed to BSS only (IMR). Moreover, compared to control females, no effect of GO was observed on CC numbers in the female fish exposed to GO by IMR (control male IMR vs. GO male IMR, $p < 0.05$; control female IMR vs GO female IMR, p = NS). In IP fish, the number of CCs, compared to controls, was significantly reduced in males exposed to GO, while in female IP fish, no significant alteration was noticed in CC numbers when compared with the corresponding control female IP fish (control male IP vs GO male IP, $p < 0.05$; control female IP vs. GO female IP, p = NS) (Fig. 7a).

3.2.3. Non-delta cells (NDC)—We have also evaluated the number of NDC (number/mm^2) in our experimental fish which have no filopodia-like process as well as negatively stained to rabbit-derived polyclonal antisomatostatin antibody. We believe that NDCs are consisting of other islet cells (α-, β-, and ε- cells) excluding δ-cells showing highest percent level (~52%) than NCDCs and CCs (Fig3b; Tables ST-1, and ST-2). Comparison of the data among different experimental groups indicated that the number of NDCs in IMR or IP female control fish are significantly higher than the corresponding control male fish in IMR and IP (control IMR male vs. control IMR female, $p<0.05$; control IP males vs. control IP females, $p<0.05$) (Fig. 7b). While the NDCs in female fish, exposed to GO by IMR are not significantly different from the corresponding male IMR fish and in IP females exposed to GO (100 μg/g) significantly reduced the number of NDCs in islet organs when compared with corresponding male IP fish (GO male IMR vs GO female IMR, p=NS; GO male IP vs. GO female IP, $p<0.05$) (Fig. 7b). Comparison between the mode of exposure (IMR vs. IP), no significant difference was observed in the number of NDCs of control IMR and IP males, but the control female IP fish showed significantly higher number of NDCs compared to IMR females exposed only to BSS (control) (control male IMR vs. control male IP, p=NS; control female IMR vs. control female IP, $p<0.05$). Also, both males and females exposed to GO by IMR did not show any significant difference with the number of NDCs than the corresponding males and females exposed to GO by IP (GO males IMR

vs. GO males IP, p=NS; GO female IMR vs. GO female IP, p=NS) (Fig7b). Finally, the effects of GO on the number of NDCs in islets of male and female fish was compared with corresponding control males and females, exposed either IMR or IP. In both male and female fish exposed to GO by IMR did not show any significant difference with the corresponding control male and female IMR fish (control male IMR vs. GO male IMR, p=NS, control female IMR vs. GO female IMR, p=NS). While in IP fish exposed to GO, the males have maintained equal status of NDCs in the islet organs with the corresponding control males (control male IP vs. GO male IP, p=NS); however, the GO-injected (100 μg/g) female fish showed significant reduction in NDC number in their islet organs when compared with corresponding vehicle-injected female fish (control) (control female IP vs. GO female IP, $p<0.05$) (Fig. 7b).

4. Discussion

The pancreas in vertebrates is an endodermal organ comprised of both exocrine and endocrine components that play a significant role in glucose metabolism. The exocrine component consists of pancreatic acinar cells that produce digestive enzymes like trypsin, amylase, elastase, and carboxypeptidase A that are transported to the digestive tract through pancreatic duct (Upchurch et al., 1994; Assouline et al., 2002; Wierup et al., 2002; Otsuka et al., 2015). The endocrine clusters, called islets, contain at least four specific types of cells, α-cells produce glucagon, β-cells produce insulin, δ-cells that produce somatostatin, and ε-cells that produce ghrelin (Upchurch et al., 1994; Wierup et al., 2002). In teleost fish, the exocrine and endocrine components of the pancreas are completely separated (Ali, 1985; Nguyen et al., 1995) and the islet tissue of many fish species are concentrated in two principal islets (Brockmanm bodies); one is found near the spleen and the other is located inside the wall of the duodenum, at the pyloric junction (Cutfield et al., 1986). In medaka, the pancreas is located dorsal to the liver, near the extrahepatic common bile duct and consists of a single large principal islet and several (2–5 in number) small secondary islets surrounded by the exocrine pancreas. The principal islet is in a more posterior region, whereas secondary islets are scattered along the gut tube, sometimes close to the bile duct (Otsuka and Takeda, 2017). These islets are comprised of insulin secreting β-cells surrounded by glucagon secreting α-cells and the hormone somatostatin secreted by δ-cells (Assouline et al., 2002; Otsuka et al., 2015; Otsuka and Takeda, 2017).

While evaluating GO as a potential EDC using Japanese medaka fish as a model, we have extended our investigations on the endocrine pancreas of medaka focusing δ-cells in the islet organs of endocrine pancreas. The rapid increase of diabetes in the modern world remains unclear and an WHO estimates that over 460 million people suffer from type 2 diabetes (T2D) (Kublbeck et al., 2020). Epidemiological data from human studies and experimental data on rodents indicate that exposure to certain EDCs may predispose patients to T2D (Ropero et al., 2008). Although graphene-based electrochemical devices could be used for diabetes monitoring and therapy (Lee et al., 2016), GO was found to be toxic in many fish models (dAmora et al., 2017; Dasmahapatra et al., 2019). However, the GO nanosheets have been documented to inhibit aggregation of amylin, a peptide deposited in the pancreas of T2D patients, and protected NIT-1 pancreatic beta cells against human islet amyloid polypeptide (hIAPP, or amylin)-induced cell death in vitro and have a possibility of using

GO in the treatment of T2D (Nedumpully-Govindan et al., 2016). In zebrafish, the damages elicited by amyloid polypeptide (IAPP) in vivo was rescued by graphene quantum dots (Wang et al., 2018). Both zebrafish and medaka have potential to regenerate pancreatic β-cells if ablated experimentally (Otsuka and Takeda, 2017). We therefore predict that endocrine pancreas in medaka could be used as an ideal organ for the evaluation of GO as an EDC.

To verify the effects on endocrine pancreas, we hypothesized that the effects of GO on the islet organs of medaka are sex-specific and depends on the route of exposure. Due to the lack of any published report, for verification of our hypothesis, we have randomly selected some experimental fish from our previous experiments (IMR fish, Dasmahapatra and Tchounwou, 2022a; b; IP fish, Dasmahapatra et al., 2020a; b). IMR fish were exposed to GO by immersion, while in IP fish, GO was administered directly to the peritoneal cavity of the fish by injection (Fig. 1). Parallel controls followed the same process of exposure without containing GO. Both IMR and IP fish were allowed for a 21 depuration/post-administration period in clean BSS (no GO) as recommended in OECD guidelines (Test No 230: 21-day Fish Assay; OECD, 2009). After 21 days postexposure, the fish were sacrificed and used standard histological techniques including immunohistochemistry for identification of specific cell types distributed in the islet organ of medaka pancreas (Figs. 2 and 3; Figs. SF-1, SF-2, SF-3). The concentration of GO we used in our IMR studies (20 mg/L) was initially based on studies made by Mullick Chowdhury et al. (2014) who exposed medaka embryos with graphene-based nanomaterials (graphene nanoribbons) for 6 consecutive days and observed significant toxicological effects; later our laboratory also confirmed by larval exposure experiments and observed significant concentration-dependent accumulation of GO/GO-like nanoparticles in the gut of the larvae (Myla et al., 2021b). For adult exposure, we followed the same exposure procedure as we did for our larval experiments and used only the highest concentration of GO (20 mg/L) we used in our previous experiments on larvae (Myla et al., 2021a,b; Asala et al., 2021, 2022). For IP exposure, we selected only 100 μg/g group for evaluation, though we have used four doses of GO (25,50, 100, and 200 μg/g) in our previous IP experiments (Dasmahapatra et al., 2020a; b). We have reason for selection of 100 μg/g dose for evaluation of pancreas, because the calculated LD_{50} of GO determined after 21 days post exposure as a breeding pair was 110.75 μg/g, which was very close or probably the maximum tolerable dose for a breeding pair for survivability and biological activity (breeding) after GO administration. The next higher dose (200 μg/g), which was the highest dose we used in the experiments, significantly affected male survivability and thus reproductive activity of the fish (Dasmahapatra et al., 2020b). Based on OECD guidelines TG230, 21-day fish assay, we have sacrificed both IMR and IP fish after 21 days post-treatment (OECD, 2009).

Our data indicated that the structure and position of the pancreas (Fig. 4), whether exocrine or endocrine, are consistent with the reports available in the literature (Assouline et al., 2002; Otsuka et al., 2015) with no potential morphological lesions on pancreatic islets were observed. In our previous IP experiments, we have observed significant accumulation of GO or GO-like nanoparticles in liver, kidney, and gonads of experimental fish and thus lesion on organs (Dasmahapatra et al., 2020a; b). In IMR experiment on adults, though our low microscopic observations did not indicate any mechanical injury in liver, kidney, gonads and

interrenal glands (adrenal homolog), the effects of GO after 21-day post exposure on internal gland indicated a probable ED effect of GO in medaka (Dasmahapatra and Tchounwou, 2022a; b). Our present study, though inconsistent, depending on the route, sex, and mode of exposure, indicated a potential ED effect of GO in medaka, probably mediated through a specific cell type found in the pancreatic islets.

To identify a specific GO-targeted cell type in islet organs of medaka, we have used standard immunohistochemical techniques using rabbit derived polyclonal antisomatostatin antibody which can specifically identify the somatostatin hormone secreting cells/organs in medaka including the δ-cells in the pancreatic islet organs. Due to unique neuron-like morphology and filopodia like-long process, δ- cells can easily differ from other islet organ cells, and their significant inhibitory role in regulating both α- (glucagon secreting) and β-cells (insulin secreting) within the islet by paracrine mechanisms, prompted us to focus our investigations on these cell types (δ-cells). During evaluation, we are concentrating on the structural and functional modifications of δ-cells induced in GO-exposed fish compared to controls. Although in teleost fish, immunohistochemical analysis identified several forms of somatostatin including somatostatin-14, −28, and 25-like peptides, encoded by two separate genes, expressed in pancreatic islets (Abad et al., 1992), the rabbit-derived polyclonal antisomatostatin antibody we have used in our studies (catalog number ab108456 Abcam, Waltham, MA) identified immunoreactive cells localized in the outer islet mantle or at the center of the principal islets and dispersed throughout the organ in secondary islets (Fig. 2). Although many cells in the principal islets are negative to immunostaining, our technique cannot differentiate immunoreactive cells into somatostatine-14, 25, or 25-like cells. We think, the polyclonal antibody (catalog number ab108456 Abcam, Waltham, MA) we used, showed significant amino acid sequence identity with the protein sequences of somatostatin-1, somatostatin-2, and somatostatin-1b reported in GenBank (ncbi.nlm.nih.gov), (50% homology with somatostatin-1, Genbank Accession XP_004084505; 29% homology with somatostatin-2, GenBank Accession XP_004084506 and 29% homology with somatostatin-1b, GenBank Accession_004070427; the BLAST search made by the Abcam technical support, technical@abcam.com) and therefore recognizing all kinds of somatostatin secreting cells as δ-cells. Based on morphology of these somatostatin-immunoreactive cells (neuron like cell soma with extended filopodia like-process) we observed in our studies, prompted us to consider these islet organ cells as δ-cells in medaka pancreas.

Our immunohistochemical observations indicated that both in control or GO-exposed IMR and IP fish, in principal islets, the immunoreactive δ-cells are distributed in the outer mantel or at the center and for secondary islets scattered throughout the islet (Fig. 2); Otsuka et al. (2015) observed that in medaka, the somatostatin producing δ-cells are located only in the central part of islets along with insulin producing β-cells and the glucagon producing α-cells are found in the periphery with no sign of immunoreactive δ-sells. In other teleost, like *Ambloplites rupestris*, the somatostatin-14 expressing D cells (δ-cells) distributed throughout the islet whereas somatostatin-25 expressing D cells (δ-cells) confined to peripheral cells (Youson et al., 2006). In mice, most of the δ-cells are in the islet cortex with few δ-cells found in the islet center, whereas in humans, δ-cells occur throughout the islet (Rorsman and Huising, 2018; Hartig and Cox, 2020).

In our studies, the antibody (catalog number ab108456 Abcam, Waltham, MA) we have used has 50% homology with somatostatin −1 and 29% homology to somatostatin-2 like and somatostatin-1b proteins, and the immunogen is within the propeptide and the somatostatin-28 positions (technical@abcam.com). We therefore predict that in medaka the immunereactive δ-cells, like *A. rupestris*, are of two types and for paracrine regulation, distributed both at the center and at the periphery of the principal islets, depending on the distribution of insulin producing β-cells (located at the center) and the glucagon producing α-cells (located at the periphery) (Otsuka et al., 2015).

We have also observed that in both male and female fish whether exposed by IMR or by IP, GO appears to be enhanced the somatostatin synthesis/content in the δ-cells in the principal islets (Figs. 5a–5h). To our knowledge, the effects of graphene-based nanomaterials on the δ-cells of pancreatic islets is not known. However, δ-cells are the paracrine regulator for inhibition of insulin synthesis in β-cells and glucagon synthesis in α-cells (Huising, 2020), therefore more data on both α- and β- cells of medaka after GO exposure is necessary. Studies indicate that graphene-based quantum dots and GO have rescued protein dysregulation of pancreatic beta cells exposed to human islet amyloid polypeptide (hIAPP/amylin), which is directly associated with the death of pancreatic β- cells and subsequent insulin deficiency in T2D (Nedumpully-Govindan et al., 2016; Wang et al., 2018; Faridi et al., 2019). Although during embryo-larval development, pancreatic β-cells in Japanese medaka rapidly regenerate after specific ablation (Otsuka and Takeda, 2017), we predict that, GO probably inhibited the synthesis of amylin/amylin-like proteins in β-cells and thus reduced the deposition of the peptide (amylin-like) on pancreas which can stimulate/activate δ-cells to secrete more somatostatin for paracrine regulation of either β- or α-cells or both.

Although δ-cells are the third highest cells in the islets, in mice, only ~6% cells are δ-cell and in human, δ-cells are more abundant (~ 22%) than mouse (Rorsman and Huising, 2018; Hartig and Cox, 2020). To observe an effect on cellular distribution, for quantitative evaluation, we have counted the δ-cells in an islet (number of cells/mm^2 of islet) and classified the islet organ cells initially into two categories; δ-cells (immunoreactive to somatostatin antibody and neuron like morphology with filopodial like processes) and NDCs (negative to immunoreactivity having round, oval, or cylindrical cell soma). The δ-cells were further classified as CC (these cells are in communication with other δ- or non- δ-cells) and the NCDC (the filopodia did not communicate with any other δ- or non- δ-cells). Based on this classification considering all 20 experimental fish, irrespective of sex, mode of exposure, or exposed to GO or not, we have observed that the population of NCDC in an islet organ is least abundant, while the number of non-delta cells is highest (Fig. 3b). Moreover, due to mixture of other non-delta cells in CCs, our studies on cell count are unable to accurately determine the number of δ-cells present in an islet organ, which seems to be higher than the number reported in mice and humans (Huising, 2020). We predict that the number of δ-cells in an islet organ of pancreas depends on the species, sex, metabolic activities, and physiological conditions of the animal (in our case all fish are adult and reproductively active). However, before drawing a definite conclusion, the counting of other islet cells (α-, β-, ε- cells) in medaka are necessary.

While counting, we have considered the nuclear area and the filopodial length of NCDC, and the cellular distribution (number/mm^2) of NCDC, CC, and NDC within an islet organ (Figs. 6 and 7). Because of the possibility of heterogeneous cell populations in CC (δ-cells and non δ-cells) and NDC (α-, β-, and other islet cells), we did not consider the nuclear area of CCs and NDCs or the filopodial length in CCs. Our data on cellular distribution of NCDC, CC, and NDC, while considering sex, route of exposure, or exposed to GO or not, were unable to establish a consistent linear effect on the islet organ of reproductively active adult male and female medaka. To establish GO as an EDC focusing endocrine pancreas of medaka as the target organ, more studies in other cell types, especially, α-, β-, and ε- cells are necessary.

5. Conclusion

Our immunohistochemical studies indicate that δ-cells in medaka adults contain somatostatin, which is increased by GO, and is potentially released directly to nearby or distant islet cells through dynamic filopodia-like processes. Like mammals, the δ-cell filopodia may release their content (somatostatin) directly in the blood/blood vessels. Also, the linear length of filopodia is highly variable, owing to the fact that all the δ-cells in an islet organ are not in communication (NCDC) with other cells at the same time. Also, not all the δ-cells in an islet organ participate in cell signaling at the same time. Moreover, exposure of Japanese medaka fish to GO either by IMR or IP, produced specific biological effects on the islet organ of pancreas. However, these effects were inconsistent, underscoring the need for using our research data to guide further studies using other cell types including the α-, β-, and ε- cells.

Supplementary Material

Refer to Web version on PubMed Central for supplementary material.

Acknowledgements

The research was supported by NIH/NIMHD grant # G12MD07581 (RCMI Center for Environmental Health), NIH/NIMHD grant #1U54MD015929 (RCMI Center for Health Disparities Research) and NSF grant #HRD 1547754 (CREST Center for Nanotoxicity Studies) at Jackson State University, Jackson, Mississippi, USA.

Data availability

Data will be made available on request.

References

Abad ME, Garcia Ayal A, Lozano MT, Agulleiro B, 1992. Somatostatin 14-and somatostatin 25-like peptides in pancreatic endocrine cells of Sparus aurrata (teleost): a light and electron microscopic immunocytochemical study. Gen. Comp. Endocrinol 86, 445–452. [PubMed: 1383077]

Ali S, 1985. Microvasculature of the pancreatic islets in the scorpion fish, Myoxocephalus scorpius. Arch Histol Jap 48, 363–371. [PubMed: 3909984]

Arrojo e Drigo R, Jacob S, Garcia-Prieto CF, Zheng X, Fukuda M, Niu HTT, Stelmashenko O, Pecanha FLM, Rodriguez-Diaz R, Bushong E, Deerinck T, Phan S, Ali Y, Leibiger I, Chua M, Boudier T, Song S-H, Graf M, Augustine GJ, Ellisman MH, Berggren P-O. Structural basis for delta cell paracrine regulation in pancreatic islets. Nat Commun. 10:3700. 10.1038/s41467-019-11517-x.

Asala TE, Dasmahapatra AK, Myla A, Tchounwou PB, 2021. Experimental data sets on the evaluation of graphene oxide as a thyroid endocrine disruptor and a modulator of gas gland cells in Japanese medaka (Oryzias latipes) larvae at the onset of maturity. Data Brief. 39, 107625 10.1016/jdib.2021.107625. [PubMed: 34901348]

Asala TE, Dasmahapatra AK, Myla A, Tchounwou PB, 2022. Histological and histochemical evaluation of graphene oxide on thyroid follicles and gas gland of Japanese medaka larvae (Oryzias latipes). Chemosphere 286, 131719 10.1016/jchemosphere.2021.131719. [PubMed: 34426126]

Assouline B, Nguyen V, Mahe S, Bourrat F, Scharfmann R, 2002. Development of the pancreas in medaka. Mech. Dev 117, 299–303. [PubMed: 12204274]

Avant B, Bouchard D, Chang X, Hsin-Se H, Acrey B, Han Y, Spear J, Zepp R, Knightes CD, 2019. Environmental fate of multiwalled carbon nanotubes and graphene oxide across different aquatic ecosystems. NanoImpact 13, 1–12. [PubMed: 31297468]

Cutfield JF, Cutfield SM, Carne A, Emdin SO, Falkmer S, 1986. The isolation, purification and aminoacid sequence of insulin from the teleost fish Cottus Scorpius (daddy sculpin). Eur. J. Biochem 158, 117–123. [PubMed: 3525155]

d′Amora M, Camisasca A, Lettieri S, Giordani S, 2017. Toxicity assessment of carbon nanomaterials in zebrafish during development. Nanomaterials 7, 414. 10.3390/nano7120414. [PubMed: 29186817]

Dasari Shreena TP, McShan D, Dasmahapatra AK, Tchounwou PB, 2018. A review on graphene-based nanomaterials in biomedical applications and risks in environment and health. Nano-Micro 10 (3), 53.

Dasmahapatra AK, Tchounwou PB, 2022a. Histopathological evaluation of the interrenal gland (adrenal homolog) of Japanese medaka (Oryzias latipes) exposed to graphene oxide. Environ. Toxicol 37, 2460–2482. DOI 10.1002/tox.23610. [PubMed: 35809259]

Dasmahapatra AK, Tchounwou PB, 2022b. Experimental data-sets on the histopathological and the immunohistochemical assessment of the interrenal gland (adrenal homolog) of Japanese medaka fish (Oryzias latipes) exposed to graphene oxide. Data Brief. 45, 108693. Doi 10.1016/j.dib.2022.108693. [PubMed: 36426008]

Dasmahapatra AK, Dasari TPS, Tchounwou PB, 2019. Graphene-based nanomaterial toxicity in fish. Rev. Environ. Int 2019 (130), 104928.

Dasmahapatra AK, Powe DK, Dasari TPS, Tchounwou PB, 2020a. Assessment of reproductive and developmental effects of graphene oxide on Japanese medaka (Oryzias latipes). Chemosphere 259, 127221. 10.1016/chemosphee.2020.127221. [PubMed: 32615454]

Dasmahapatra AK, Powe DK, Dasari TPS, Tchounwou PB, 2020b. Experimental data sets on the characterization of graphene oxide and its reproductive and developmental effects on Japanese medaka (Oryzias latipes) fish. Data Brief. 32, 106218 10.1016/j.dib.2020.10628. [PubMed: 32939377]

De Marchi L, Pretti C, Gabriel B, Marques PAAP, Freitas R, Neto V, 2018. An overview of graphene materials: properties, applications and toxicity on aquatic environments. Sci. Total Environ 631–632, 1440–1456.

Faridi A, Sun Y, Mortimer M, Aranha R, Nandakumar A, Li Y, Javed I, Kakinen A, Fan Q, Purcell AW, Davis TP, Ding F, Faridi P, Ke PC, 2019. Graphene quantum dots rescue protein dysregulation of pancreatic β- cells exposed to human islet amyloid polypeptide. Nano Res. 12, 2827–2834. [PubMed: 31695851]

Fernandez L, 2022. Graphene industry worldwide- statistics &facts. 〈https://www.statista.com/topics/8769/graphene-industry-world-wide/#topicHeader_wrapper〉.

Gao R, Yang T, Zhang Q, 2021. δ-cells: the neighborhood watch in the islet community. Biology 2021 (10), 74. 10.3390/biology10020074.

Han Y, Knightes CD, Bouchard D, Zeep R, Avant B, Hsieh H-S, Chang X, Acrey B, Henderson H, Spear J, 2019. Simulating graphene oxide nanomaterial phototransformation and transport in surface water. Environ. Sci. Nano 6, 180–194. [PubMed: 31297195]

Hartig SM, Cox AR, 2020. Paracrine signaling in islet function and survival. J. Mol. Med 98, 451–467. [PubMed: 32067063]

Huising MO, 2020. Paracrine regulation of insulin secretion. Diabetologia 63, 2057–2063. [PubMed: 32894316]

Karthikeyan BS, Ravichandran J, Mohanraj K, Vivek-Anath RP, Samal A, 2019. A curated knowledgebase on endocrine disrupting chemicals and their biological systems-level perturbations. Sci. Total Environ 692, 281–296. [PubMed: 31349169]

Krimsky S, 2017. The unsteady state and inertia of chemical regulation under the US toxic substances control act. PLos Biol. 2017 (15), e2002404.

Kublbeck J, Vuorio T, Niskanen J, Fortino V, Braeuning A, Abass K, Rautio A, Hakkola J, Honkakoski P, Levonen A-L, The EDCMET project: Metabolic effects of endocrine disruptors. Int. J. Mol Sci 21(8)3021.doi.10.3390/ijms21083021.

Lee H, Choi TK, Lee YB, Cho HR, Ghaffari R, Wang L, Choi HJ, Chung TD, Lu N, Hyeon T, Choi SH, Kim D-H, 2016. A graphene-based electrochemical device with thermoresponsive microneedles for diabetes monitoring and therapy. Nat. Nano 11, 566–572.

Li D, Wang T, Li Z, Xu X, Wang C, Duan Y, 2020. Application of graphene-based materials for detection on nitrate and nitrite in water-a review. Sensors 20 (54). 10.3390/s20010054.

Mullick Chowdhury S, Dasgupta S, McElroy AE, Sitharaman B, 2014. Structural disruption increases toxicity of graphene nanoribbons. J. Appl. Toxicol 34, 1235–1246. [PubMed: 25224919]

Myla A, Dasmahapatra AK, Tchounwou PB, 2021a. Sex-reversal and histopathological assessment of potential endocrine disrupting effects of graphene oxide on Japanese medaka (Oryzias latipes) larvae. Chemosphere 221 (279), 130768. 10.1016/j.chemosphere.2021.130768.

Myla A, Dasmahapatra AK, Tchounwou PB, 2021b. Experimental data sets on sex-reversal and histopathological assessment of potential endocrine disrupting effects of graphene oxide on Japanese medaka (Oryzias latipes) larvae at the onset of maturity. Data Brief. 38, 107330 http//10.1016/j.dib.2021.107330. [PubMed: 34504916]

Nedumpully-Govindan P, Gurzov EN, Chen P, Pilkington EH, Stanley WJ, Litwak SA, Davis TP, Ke PC, Ding F, 2016. Graphene oxide inhibits hIAPP amyloid fibrillation and toxicity in insulin-producing NIT-1 cells. Phys. Chem. Chem. Phys 18, 94–100. [PubMed: 26625841]

Nguyen TM, Wright JR Jr, Nielsen PF, Conlon JM, 1995. Characterization of the pancreatic hormones from the Brockmann body of the tilapia: implications for islet xenograpts studies. Comp. Biochem Physiol. Part C. ; Pharmacol. Toxicol. Endocrinol 111, 33–44.

OECD, 2009. OECD guidelines for the testing of chemicals; 21-day fish assay: a short-term screening for oestrogenic and androgenic activity, and aromatase inhibition. org/environment/test-no-230-21-day-fishassay_9789264076228-en.OECD-library,.

OECD, 2018. Revised guidance document 150 on standardized test guidelines for evaluating chemicals for endocrine disruption. OECD series on testing and assessment. OECD publishing, Paris, p. 2018. 10.1787/9789264304741-en.

Otsuka T, Takeda H, 2017. Targeted ablation of pancreatic βcells in medaka. Zool. Sci 34, 179–184.

Otsuka T, Tsukahara T, Takeda H, 2015. Development of the Pancreas in medaka, Oryzias latipes, from embryo to adult. Dev. Growth Differ 57, 557–569. [PubMed: 26435359]

Readman GD, Owen SF, Knowles TG, Murrell JC, Species specific anesthetics for fish anesthesia and euthanasia. Sci Rep 7:7102. Doi:10.1038/s41598-01706917-2.

Ropero AB, Alonso-Magdalena P, Garcia-Garcia E, Ripoll C, Fuentes E, Nadal A, 2008. Bisphonal-A disruption of the endocrine pancreas and blood glucose homeostatic. Int J. Androl 31, 194–200. [PubMed: 17971160]

Rorsman P, Huising M, 2018. The somatostatin-secreting pancreatic δ-cells in health and disease. Nat. Rev. Endocrinol 14, 404–414. 10.1038/s41574-018-0020-6. [PubMed: 29773871]

Seralini GE, Jungers G, 2021. Endocrine disruptors also function as nervous disruptors and can be renamed endocrine and nervous disruptors. Toxi. Rep 8, 1538–1557.

Upchurch BH, Aponte GW, Leiter AB, 1994. Expression of peptideYY in all four islet cell types in the developing mouse pancreas suggests a common peptide YY-producing progenitor. Development 120, 245–252. [PubMed: 8149907]

Wang M, Sun Y, Cao X, Peng G, Javed I, KakinenDavis TP, Lin S, Liu J, Ding F, Ke PC, 2018. Graphene quantum dots against human IAPP aggregation and toxicity in vivo.

Wierup N, Svensson H, Mulder H, Sundler F, 2002. The ghrelin cells: a novel developmentally regulated islet cell in the human pancreas. Regul. Papt 107, 63–69.

Youson JH, Al-Mahrouki AA, Amemiya Y, Graham LC, Montpetit CJ, Irwin DM, 2006. The fish endocrine pancreas: review, new data, and future research directions in ontogeny and phylogeny. Gen. Comp. Endocrinol 148, 105–115. [PubMed: 16430894]

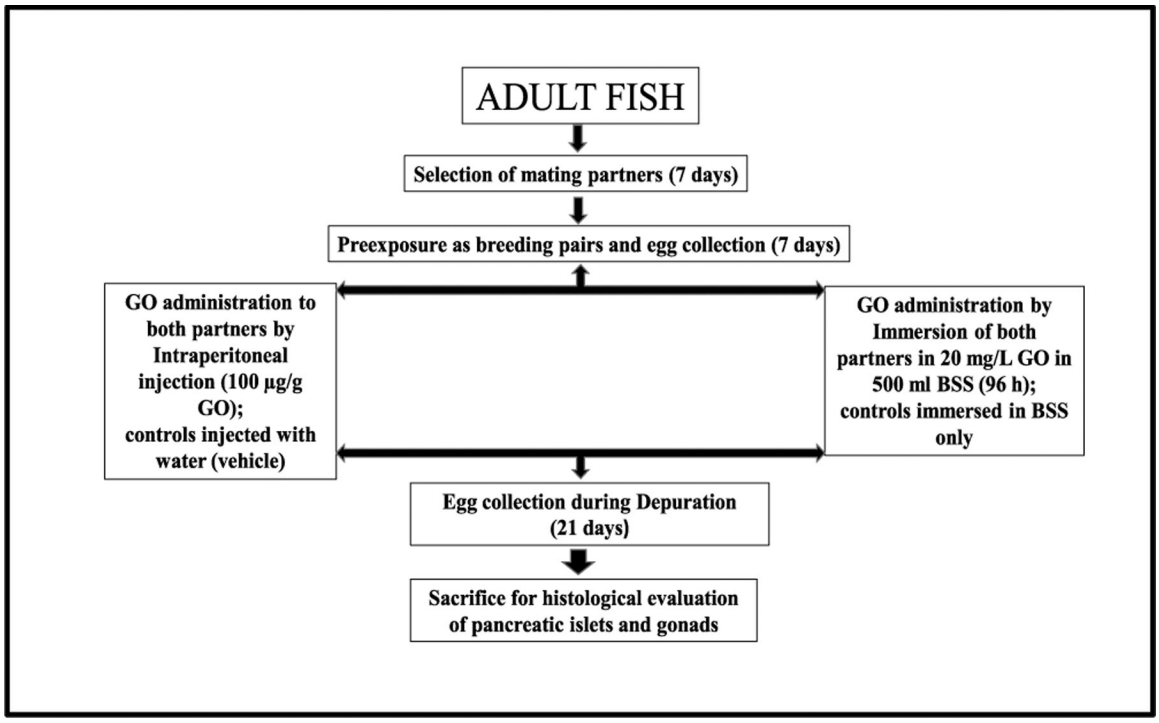

Fig. 1. Schematic diagram of the GO exposure paradigm to adults of Japanese medaka fish.

Sexually mature, reproductively active, adult male and female medaka fish as a breeding pair (one male and one female) were maintained in 500 mL BSS in a one L glass jar in standard laboratory conditions (light cycle: 16 h light 8 h dark; 25 ± 1 °C). Eggs were collected (both fertilized and unfertilized) for 7 consecutive days before the exposure to GO either by IMR (20 mg/g; 96 h continuous with refreshing of media every 24 h) or by IP-injection (100 µg/g; single injection). Food was given to adult fish during the exposure period. Control fish were immersed in 500 mL BSS or injected with vehicle (water). The media was refreshed every day. After GO exposure (either by IMR or IP) the fish were transferred to 500 mL of fresh BSS (no GO) and allowed breeding (same pair) and maintained 21 days in a GO-free environment with regular feeding and refreshing of media (BSS). The collection of eggs from individual breeding pair continued. On 21st day post-treatment (3 weeks depuration) the fish were sacrificed, and the trunk region was preserved in 4% PFA in 20 mM PBS for histological/immunohistochemical examination of the islet tissue.

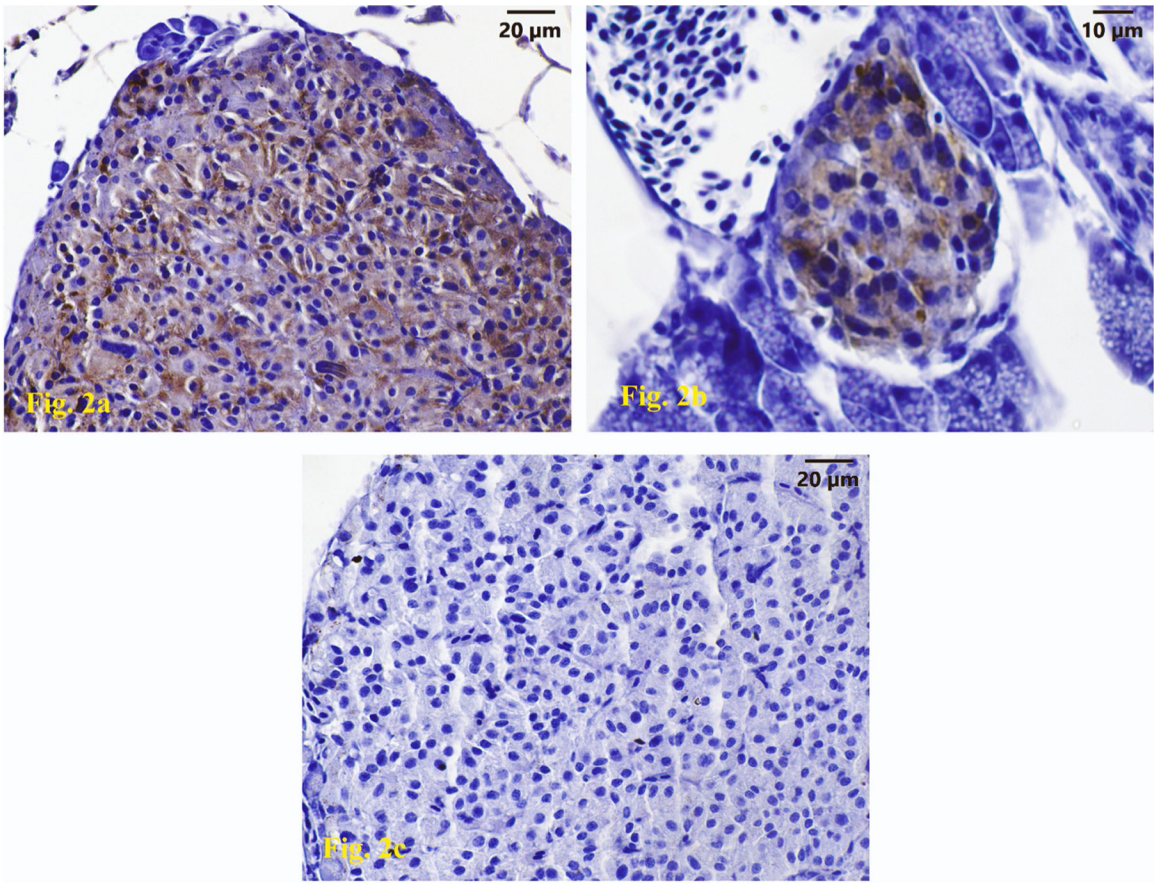

Fig. 2.

Representative photomicrographs showing immunohistochemical staining of the pancreatic islets of Japanese medaka adults, counterstained with hematoxylin. Fig. 2a: principal islet with primary antibody; 2b: secondary islet with primary antibody; 2c principal islet without primary antibody.

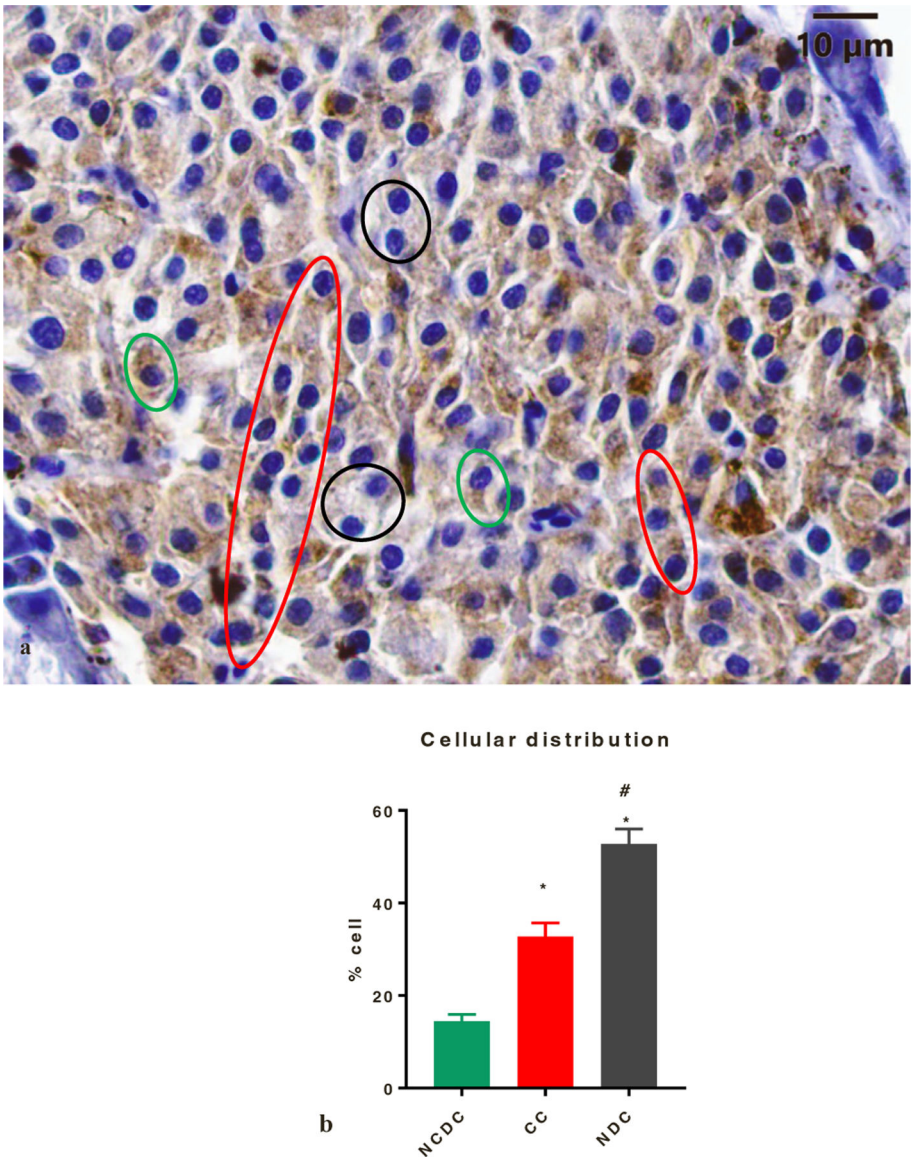

Fig. 3.

Representative photomicrograph of a principal islet of an adult medaka fish immunostained with rabbit antisomatostatin antibody (Abcam, Waltham, MA) and counterstained with hematoxylin. Fig. 3a showing three different types of islet organ cells considered for evaluation. Cells within green circles indicate noncommunicating δ-cells (NCDC), cells within red circles indicate communicating cells (CC), and cells within black circles indicate non- δ-cells (NDC). Fig. 3b showed the per cent (%) distribution of all these three cell types (NDC, CC, and NCDC) within an islet organ/tissue. The bar head with asterisks indicate significant difference ($p < 0.05$) with NCDC and with # symbol indicate significant difference ($p < 0.05$) with CC.

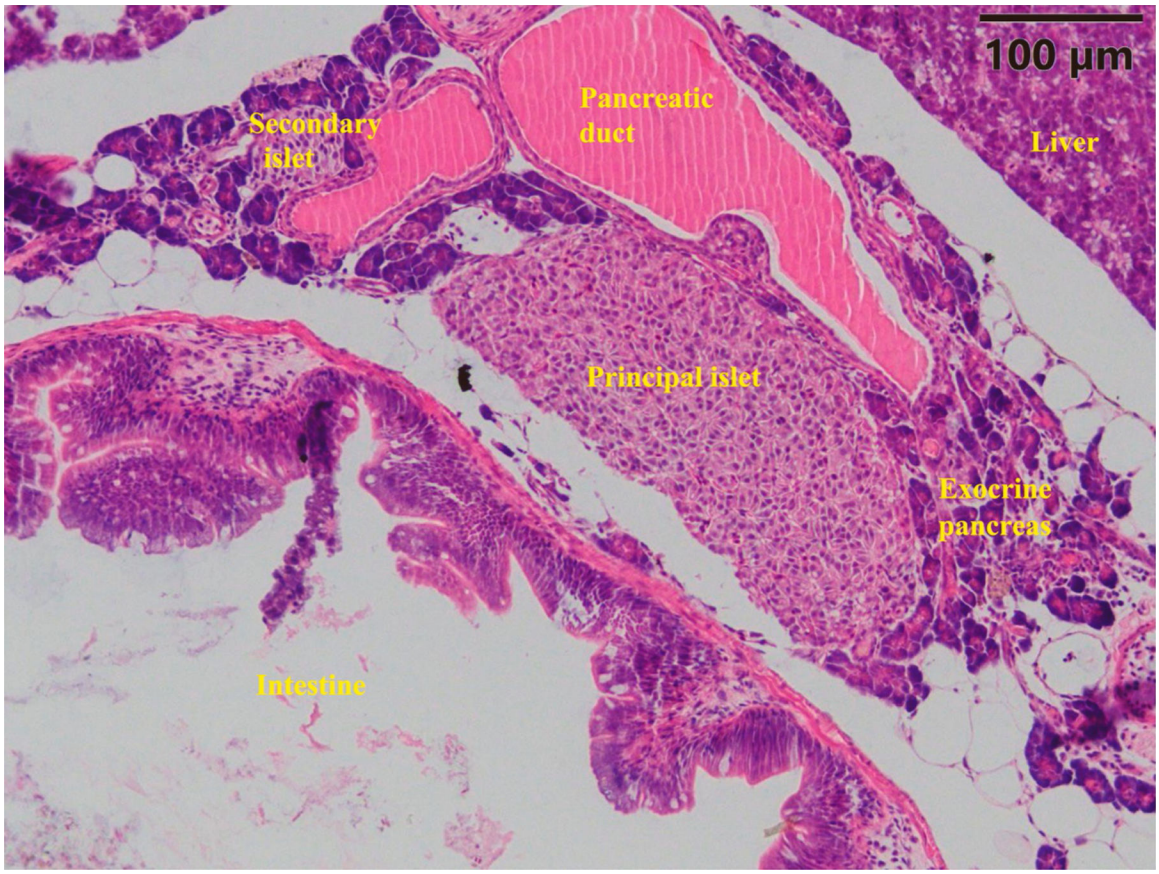

Fig. 4.

Representative Figure in HE staining showing the location of pancreatic islet organs in an adult medaka.

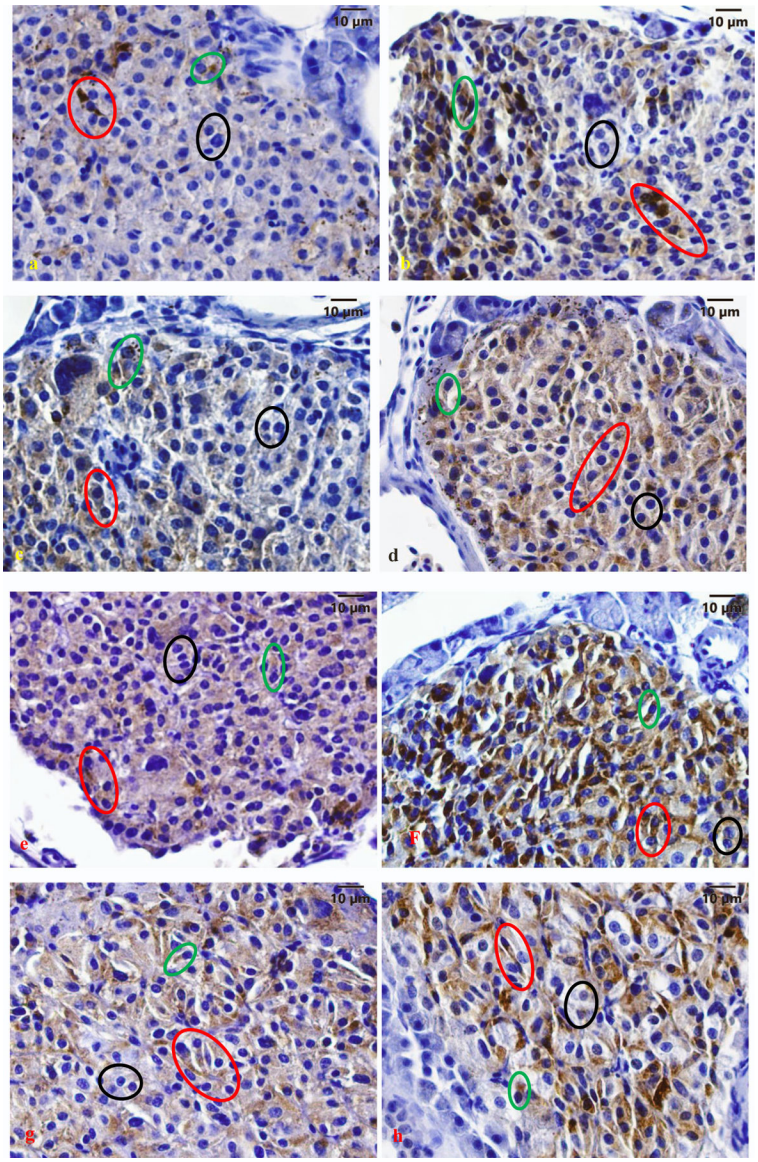

Fig. 5.

Representative Figures showing immunoreactive (antisomatostatin antibody positive) δ-cells in the islet organs of medaka adult fish exposed to GO either by IMR (20 mg/L; Figs. 5b, 5d) or by IP (100 µg/g; Fig. 5 f, 5 h). Parallel control fish (no GO; Figs. 5a, 5c) in IMR experiments exposed to BSS only. Control fish (Figs. 5e, 5g) in IP experiments injected with nanopure water. Figs. 5a, 5b, 5e, 5h= male fish; Figs. 5c, 5d, 5g, 5h= female fish. The cells encircled by green circles represent noncommunicating δ-cells (NCDC), by red circles indicate communicating cells (CC) and by black circles are non-δ cells (NDC).

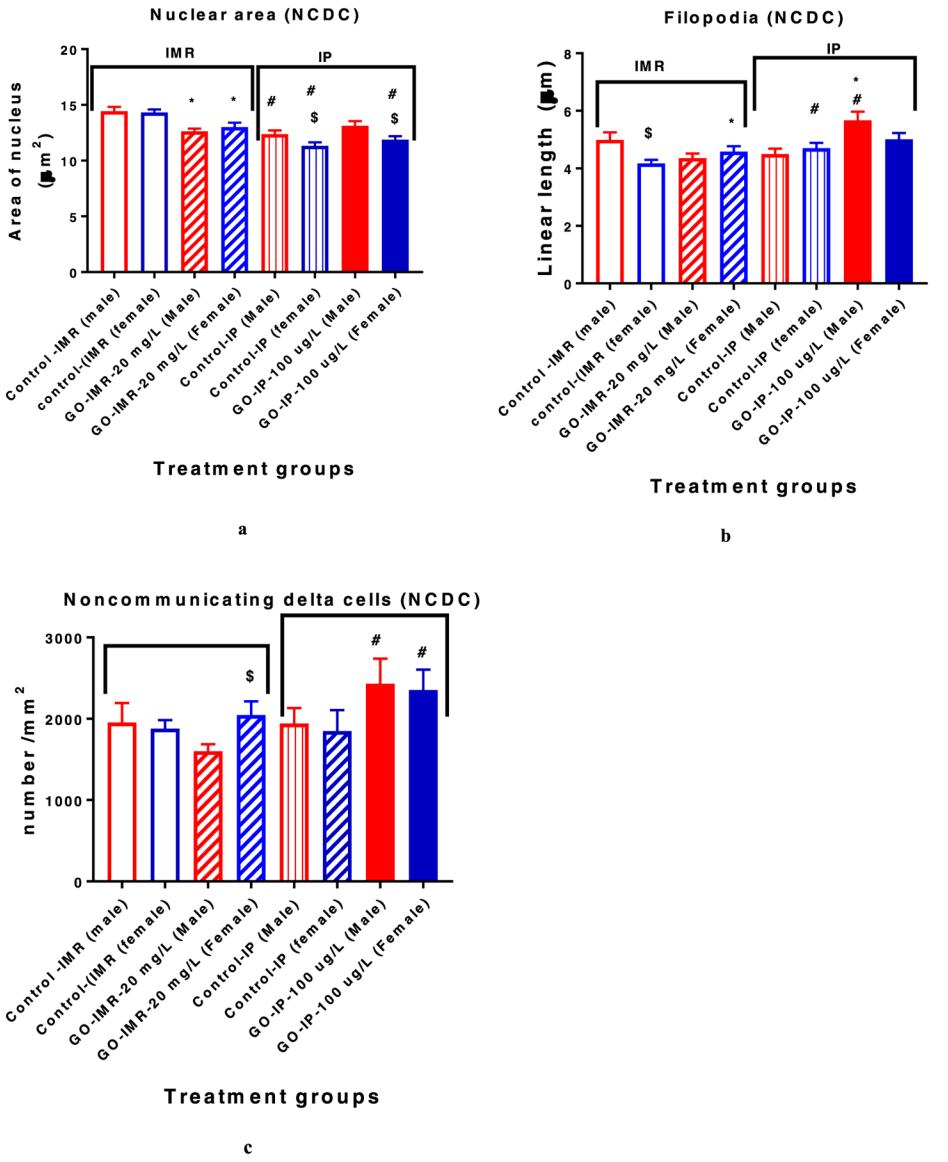

Fig. 6. : The noncommunicating delta cells (NCDC) in the islet organ of Japanese medaka adults after GO exposure.

Reproductively active adult male and female Japanese medaka as breeding pair were exposed to GO either by IMR (20 mg/L) continuously for 96 h in BSS or by IP (100 μg/g). Controls in IMR fish were maintained in BSS only and for IP experiments were vehicle-injected (nanopure water, 1 μL/10 mg body weight) and maintained in BSS. The fish, after GO treatment were maintained in a GO-free environment in the laboratory for 21 days and sacrificed for immunohistological evaluation of the islet cells using rabbit derived polyclonal antisomatostatin antibody. Fig. 6a= nuclear area of NCDC; Fig. 6b= linear length of filopodia in NCDC; Fig. 6c= number of NCDC (/mm^2) within an islet organ are presented. Each bar represents the mean ± SEM. The bar heads with asterisks (*) represent significant difference between control fish (males or females) with corresponding males or female fish exposed to GO either by immersion (IMR) or by intraperitoneal injection (IP). Bar heads with # symbol indicate significant difference between mode of exposure (IMR

vs. IP) of the male or female fish exposed as control or GO. Symbol $ is used to indicate significant difference between the sex of the fish (male vs female) exposed either as control or to GO (IMR or IP).

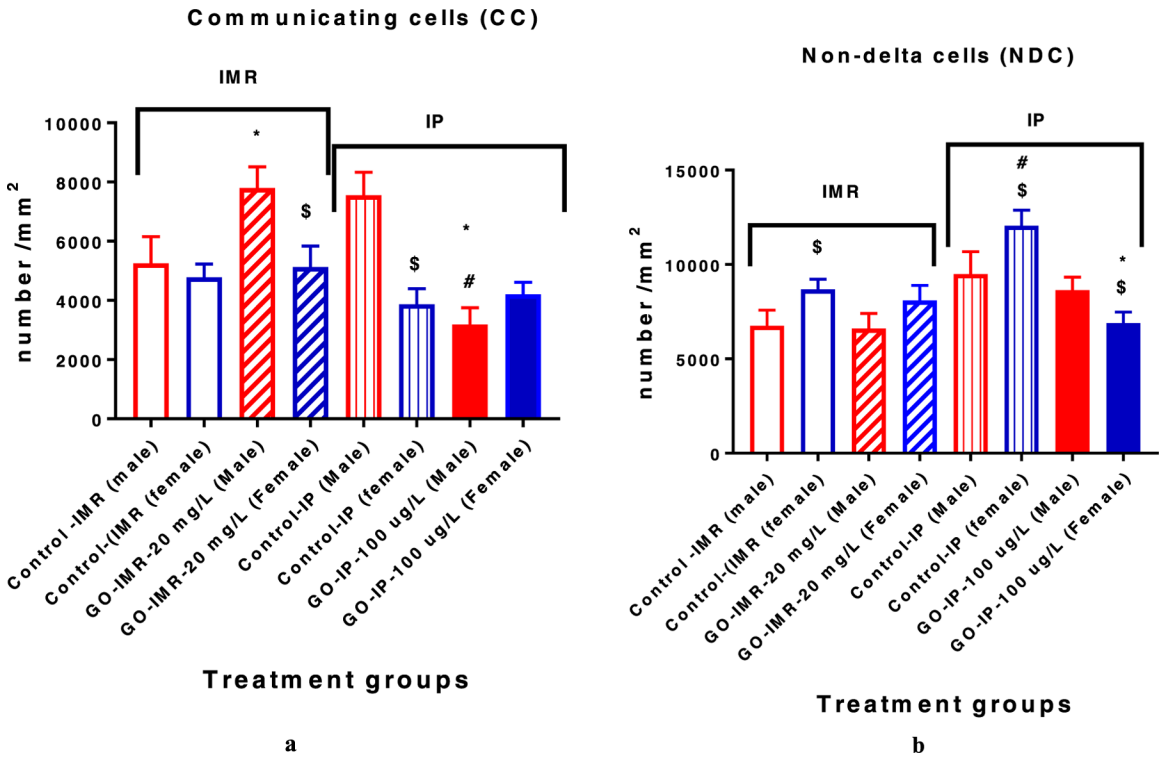

Fig. 7. : Cellular distribution of the communicating cells (CCs) and the non-delta cells (NDCs) in the islet organ of Japanese medaka adults after GO exposure.

Reproductively active adult male and female Japanese medaka as breeding pairs were exposed to GO either by IMR (20 mg/L continuously for 96 h in BSS) or by IP (100 μg/g). Controls in IMR fish were maintained in BSS only and for IP experiments were vehicle-injected (nanopure water) and maintained in BSS. The fish, after GO treatment were maintained in a GO-free environment in the laboratory for 21 days and sacrificed for immunohistological evaluation of the islet cells using rabbit derived polyclonal antisomatostatin antibody. Fig. 7a= CC; Fig. 7b= NDC. Each bar represents the mean ± SEM. The bar heads with asterisks (*) represent significant difference between control fish (males or females) with corresponding males or female fish exposed to GO either by immersion (IMR) or by intraperitoneal injection (IP). Bar heads with # symbol indicate significant difference between the mode of exposure (IMR vs. IP) of the male or female fish exposed as control or GO. Symbol $ is used to indicate significant difference between the sex of the fish (male vs female) exposed either as control or to GO (IMR or IP).